Mon. Not. R. Astron. Soc. **000**, 000–000 (0000) Printed 1 February 2008 (MN LATEX style file v1.3)

A Multiphase Model for the Intracluster Medium

Daisuke Nagai[1], Martin E. Sulkanen[2,3], and August E. Evrard[1]
[1] *Physics Department, University of Michigan, Ann Arbor, MI 48109–1120 USA*
[2] *X-Ray Astronomy Group, Space Sciences Laboratory, NASA/Marshall Space Flight Center, Huntsville, AL 35812 USA*
[3] *Present address: Astronomy Department, University of Michigan, Ann Arbor, MI 48109–1090 USA*
daisuken@umich.edu
msulkanen@astro.lsa.umich.edu
evrard@boris.physics.umich.edu

1 February 2008

ABSTRACT

Constraints on the clustered mass density Ω_m of the universe derived from the observed population mean intracluster gas fraction $\langle f_{ICM} \rangle$ of X–ray clusters may be biased by reliance on a single-phase assumption for the thermodynamic structure of the intracluster medium (ICM). We propose a descriptive model for multiphase structure in which a spherically symmetric ICM contains isobaric density perturbations with a radially dependent variance $\sigma^2(r) = \sigma_c^2(1 + r^2/r_c^2)^{-\epsilon}$. The model extends the work of Gunn & Thomas (1996) which assumed radially independent density fluctuations thoughout the ICM.

Fixing the X–ray emission profile and emission weighted temperature, we explore two independently observable signatures of the model in the $\{\sigma_c, \epsilon\}$ space. For bremsstrahlung dominated emission, the central Sunyaev–Zeldovich (SZ) decrement in the multiphase case is increased over the single-phase case and multiphase X–ray spectra in the range $0.1 - 20$ keV are flatter in the continuum and exhibit stronger low energy emission lines than their single-phase counterpart. We quantify these effects for a fiducial 10^8 K cluster and demonstrate how the combination of SZ and X–ray spectroscopy can be used to identify a preferred location $\{\hat{\sigma}_c, \hat{\epsilon}\}$ in the model plane. From these parameters, the correct value of $\langle f_{ICM} \rangle$ in the multiphase model results, allowing an unbiased estimate of Ω_m to be recovered.

The consistency of recent determinations of the Hubble constant from SZ and X–ray observations with values determined by other methods suggests that biases in ICM gas fractions are small, $\lesssim 20\%$.

Key words: single-phase ICM – multi-phase ICM – clusters: galaxies

1 INTRODUCTION

The existence of non-baryonic or "dark" matter on very large scales in the universe is inferred from a number of observations, including X–ray and gravitational lensing observations of galaxy clusters. Observations suggest that the baryonic component of clusters predominantly consists of hot, diffuse, intergalactic medium (ICM) which emits X–rays by scattering of electrons in the Coulomb fields of electrons and ions, *i.e.*, thermal bremsstrahlung. The X–ray observations determine the ICM mass content in a model dependent fashion. Recent analysis of the flux limited Edge sample employs the standard, isothermal β–model and finds a mean ICM mass fraction $\langle f_{ICM} \rangle = 0.212 \pm 0.006$ (Mohr, Mathiesen & Evrard 1998; see also White & Fabian 1996; David, Forman & Jones 1996) within the virial regions of 27 nearby clusters with X–ray temperatures above 5 keV. This value is several times larger than that expected in an Einstein–deSitter universe with the observed light element abundances (White et al. 1993).

One way to reconcile the cluster observations with a universe having critical mass density $\Omega_m = 1$ is to suspect that the standard model treatment of the ICM posseses substantial systematic errors. Gunn & Thomas (1996, hereafter GT96), motivated by models of cooling flows (Nulsen 1986; Thomas 1988) propose that a multi-phase ICM structure ex-

ists throughout the cluster atmosphere. A given macroscopic volume element contains gas at a range of densities and temperatures which are assumed to be in pressure equilibrium. Fixing the gas mass within this volume, the emission measure of a multiphase gas will increase as the clumping factor $C \equiv \langle \rho^2 \rangle / \langle \rho \rangle^2$. But since we observe luminosity, not gas mass, the implication is that clumped gas requires less total mass $M_{gas} \propto 1/\sqrt{C}$ in a given volume to produce a fixed X–ray emissivity.

The standard analysis of the cluster plasma assumes that it exists in a single thermodynamic phase at any location within the cluster. In most cases an isothermal, "beta" model (Cavaliere & Fusco-Femiano 1976) is used to describe the cluster plasma electron density for a spherically symmetric atmosphere. Under these assumptions, the observed azimuthal X–ray surface brightness profile determines the volume emissivity at radius r from the cluster center

$$\xi(r) \equiv \rho^2(r)\Lambda_X(T_X) = \xi_0 \left(1 + \frac{r^2}{r_c^2}\right)^{-3\beta+\frac{1}{2}}. \quad (1)$$

Here ξ_0 is the central value of the X–ray emissivity, r_c is the core radius of the X–ray emission, $\Lambda_X(T_X)$ is the (suitably normalized) plasma emission function at a temperature T_X over a prescribed X–ray bandwidth. The temperature T_X is determined from X–ray spectral measurements by, for example, fitting the observed spectrum to a thermal bremsstrahlung model. With observations and plasma emission model in hand, one then constructs the gas mass density $\rho(r) = (\xi_0/\Lambda_X(T_X))^{1/2}(1 + r^2/r_c^2)^{-3\beta/2}$ and integrates outward from the origin to define enclosed gas mass.

The total (baryonic plus non-baryonic) mass within a radius r is inferred from assuming that the plasma is in hydrostatic equilibrium, supported against gravity entirely by thermal pressure. The fluid equation of hydrostatic equilibrium then sets the total, gravitating mass

$$M_{\rm tot}(r) = -\frac{r^2}{G}\frac{1}{\rho}\frac{dP}{dr}, \quad (2)$$

which for the fiducial, single-phase, isothermal β–model cluster gives

$$M_{\rm tot,s}(r) = \frac{3\beta}{G}\frac{k_B T_X}{\mu m_p}\frac{r^3/r_c^2}{1 + r^2/r_c^2}. \quad (3)$$

In this paper, we extend a multiphase ICM model first proposed by Gunn & Thomas (1996, herafter GT96) to incorporate radial variability in the multiphase structure. Radial variability is a natural expectation. Since both cooling timescales ($\propto \rho^{-1}$ if nearly isothermal) and local gravitational timescales ($\propto \rho^{-1/2}$) increase outward from the cluster core, the timescale for development of multiphase structure should also be larger at the virial surface than in the core of a cluster.

We introduce the theoretical model in §2 below. In §3, we examine the effects of a multiphase structure on the mean intracluster gas fraction $\langle f_{ICM} \rangle$ inferred from X–ray observations and consider observable implications for the Sunyaev–Zeldovich (SZ) effect and X–ray spectroscopy of the ICM. For the latter, we examine two specific signatures — the excess (relative to the single-phase case) in central SZ decrement and an X-ray spectral hardness ratio — for the case of a "Coma-like" cluster. We show how the pairing of X–ray spectroscopy and SZ image can be used to estimate the magnitude of systematic error introduced into estimates of ICM gas fraction by assuming the standard β–model .

2 THEORY

GT96 argue that if a spectrum of plasma density fluctuations were generated in a cluster at a substantial fraction of a Hubble time in the past, then its densest phases would cool and be removed from the plasma. Following Nulsen (1986), they argued that this would produce a power-law spectrum of fluctuations $f(\rho) \propto \rho^{-\gamma}$ at the present, formed from a narrow range of phases that were initially tuned to have cooling times comparable to a Hubble time. However, this argument ignores the stochastic nature of gravitational clustering in hierarchical models of structure formation. In such models, clusters grow largely by mergers of proto-cluster candidates embedded within the large–scale filamentary network. It is suspected that strong mergers may, through plasma turbulence, effectively "reinitialize" density fluctuations in the ICM. Since the time since the last major merger is a random variable in a coeval population, then a volume limited sample will contain clusters whose multi-phase structures are at different stages of development. This idea is consistent with observed properties of the local X–ray cluster population, in which a range of central cooling flow behavior is present (Fabian 1994).

Because of this and other uncertainties in the dynamical development of multiphase structure, we postulate a log-normal form for the multiphase density perturbations. We do not attempt a formal justification for this choice; it is motivated largely by a condition of "reasonableness" and the fact that it simplifies calculations below. The formalism requires only low order moments of the distribution, so the model can be recalculated for arbitrary $f(\rho)$.

We postulate the existence of plasma density fluctuations in a spherically symmetric cluster atmosphere which: (i) are isobaric at a given radius, (ii) produce a volume emission profile consistent with equation (1) and (iii) exhibit an isothermal emission weighted temperature with radius. The first item is based on a hydrostatic assumption and the remainder impose observed constraints on the X–ray image and emission weighted temperature profile. Although isothermality extending to r_{200} — the radius within which the mean total mass density is 200 times the critical density — may not be supported by observations (Markevitch et al. 1998) or simulations (Frenk et al. 1998), temperature drops of only $10 - 20\%$ are allowed within $r_{200}/3$ (Irwin, Bregman & Evrard 1998). Since the observables we stress in the analysis are core dominated, our results are not particularly sensistive to departures from isothermality which may exist near r_{200}.

2.1 The multiphase distribution function

We assume a log-normal form for the cluster plasma density phase distribution $f(\rho)\,d\rho$, the fraction of a volume element at a radius r that contains plasma of density of between ρ and $\rho + d\rho$,

$$f(\rho)\,d\rho = \frac{1}{\sqrt{2\pi}\,\sigma(r)} \exp\left(- \frac{\ln^2[\rho/\rho_0(r)]}{2\sigma^2(r)} \right) \frac{d\rho}{\rho}. \quad (4)$$

The quantity $\rho_0(r)$ is a reference density and $\sigma^2(r)$ is the variance of the distribution. Since the core radius presents a characteristic scale in the X–ray image, we take a form

$$\sigma^2(r) = \sigma_c^2 (1 + r^2/r_c^2)^{-\epsilon}, \quad (5)$$

for the variance, with r_c the core radius of the beta-model density profile described earlier, and σ_c and ϵ are free parameters which set the magnitude and radial dependence of the multiphase structure. We consider such a parameterization in order to couple the magnitude of density fluctuations to the likelihood that the local conditions have allowed cooling to amplify them. A simple parameterization is one in which the variance scales with the inverse of the local cooling time $\sigma^2(r) \propto \tau_{\rm cool}^{-1}(r)$. An isothermal atmosphere (for which $\tau_{\rm cool}(r) \propto \rho^{-1}(r)$) will have $\sigma^2(r) \propto \rho(r)$, implying $\epsilon = 3\beta/2 = 1$ for the characteristic $\beta = 2/3$ value seen in X–ray images. We consider values in the range $\epsilon \in 0 - 1$. The limit $\epsilon \rightarrow \infty$ represents a multiphase structure existing purely within the cluster core. In the limit $\sigma_c \rightarrow 0$, we recover a single-phase plasma for any value of ϵ, while the limit $\epsilon \rightarrow 0$ yields the multiphase model results (no position dependence) of GT96.

The definition of $\rho_0(r)$ is now absorbed into the specification of the mean density at radius r

$$\langle \rho(r) \rangle \equiv \int \rho\, f(\rho)\, d\rho = \rho_0 \exp\left(\frac{1}{2}\sigma^2(r) \right), \quad (6)$$

where $\langle\rangle$ represents an ensemble average of volume elements on a spherical shell of radius r. A useful equation is a generalization of equation (6) to higher moments, namely

$$\langle \rho^q \rangle = \int \rho^q\, f(\rho)\, d\rho = \langle \rho \rangle^q \exp\left(\frac{q(q-1)}{2}\sigma^2(r) \right). \quad (7)$$

2.2 A multiphase "isothermal β–model " cluster

We now impose some observational constraints on the model. Assuming a power–law emissivity function

$$\Lambda_X(T) \propto T^\alpha, \quad (8)$$

the requirement that the emission weighted temperature profile be isothermal at temperature T_X implies that the condition

$$T_X \equiv \frac{\langle \rho^2 T^{1+\alpha} \rangle}{\langle \rho^2 T^\alpha \rangle} \quad (9)$$

holds at all cluster radii.

Under an ideal gas assumption $P = (\rho/\mu m_p) k_B T$, with m_p the proton mass and μ the mean molecular weight, equations (9) and (7) can be used to define the local gas pressure in the multiphase medium

$$P(r) = \frac{k_B T_X}{\mu m_p} \langle \rho(r) \rangle \, \exp[(1-\alpha)\sigma^2(r)]. \quad (10)$$

We now equate the known emission profile of the cluster, equation (1), to the ensemble-averaged value of the emissivity

$$\xi_0 \big(1 + \frac{r^2}{r_c^2}\big)^{-3\beta} = \frac{\Lambda_0}{m_p^2} \big(\frac{\mu m_p}{k_B}\big)^\alpha \langle \rho(r)^{2-\alpha} \rangle P^\alpha(r). \quad (11)$$

The combination of equations (9) and (11) is the canonical "isothermal β–model " assumption. From an observer's perspective, a multiphase cluster in these two measures is indistinguishable from the single-phase case. Equation (11) can be rearranged to give

$$\langle \rho(r) \rangle = \left(\frac{\xi_0 m_p^2}{\Lambda_X(T_X)} \right)^{1/2} \left(1 + \frac{r^2}{r_c^2} \right)^{-\frac{3}{2}\beta} \exp\big(\frac{(\alpha-1)(\alpha+2)}{4} \sigma^2(r) \big). \quad (12)$$

Although this now defines the characteristic density ρ_0 used in equation (4), it is better to identify the limit $\sigma^2(r) \rightarrow 0$ as the single-phase density. Following GT96, we introduce a multiphase "correction factor" for the gas mass $C_\rho(r)$ which relates the mean gas density in the multiphase case $\rho_m(r)$ to its single-phase value $\rho_s(r)$

$$\rho_m(r) \equiv \langle \rho(r) \rangle \equiv C_\rho(r) \rho_s(r). \quad (13)$$

Equation (12) then implies

$$C_\rho(r) = \exp\big(\frac{(\alpha-1)(\alpha+2)}{4} \sigma^2(r) \big). \quad (14)$$

A similar exercise for the gas pressure

$$P(r) \equiv C_P(r) \big(\frac{k_B T_X}{\mu m_p} \big) \rho_s(r) \quad (15)$$

yields

$$C_P(r) = \exp\big(\frac{(1-\alpha)(2-\alpha)}{4} \sigma^2(r) \big). \quad (16)$$

Note that for values of the X–ray emission exponent $\alpha < 1$, the multiphase gas mass is lower than that of the single-phase model while the multiphase pressure is greater than the single-phase pressure. This arises because the high-density phases are more efficient in producing a given X–ray power (provided the emission is only a weak function of temperature). Since the emission weighted T_X reflects the temperature in higher than average density regions, the pressure at all radii is increased over the single-phase case.

The cluster gas mass for the multiphase model within a radius r is given by

$$M_{\rm gas,m}(r) = 4\pi \int_0^r C_\rho(r')\, \rho_s(r')\, r'^2 dr', \quad (17)$$

so that the enclosed gas mass for the multiphase model differs from the single-phase case by the factor

$$C_{\rm gas}(r) \equiv \frac{M_{\rm gas,m}(r)}{M_{\rm gas,s}(r)} = \frac{\int_0^r C_\rho(r')\, \rho_s(r')\, r'^2 dr'}{\int_0^r \rho_s(r')\, r'^2 dr'}. \quad (18)$$

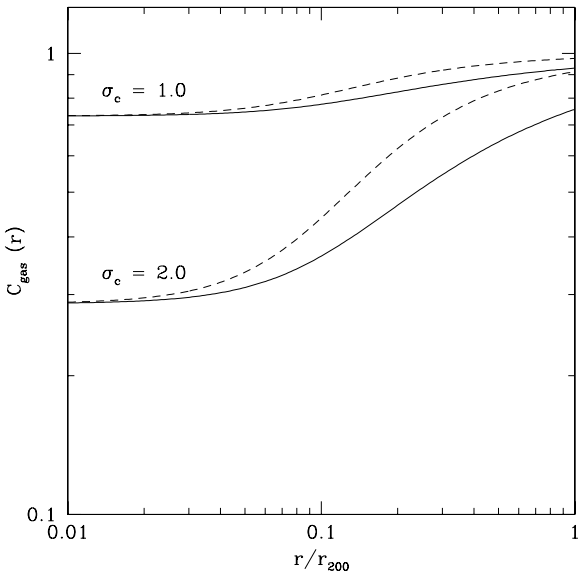

Figure 1. The gas mass multiphase correction factor $C_{gas}(r)$, equation (18), is plotted as a function of the dimensionless radius r/r_{200} assuming parameters $r_c/r_{200} = 0.1$, $\alpha = 1/2$ and $\beta = 2/3$. The solid and dotted lines represent $\varepsilon = \frac{1}{2}$ and $\varepsilon = 1.0$, respectively, and values of σ_c are as indicated.

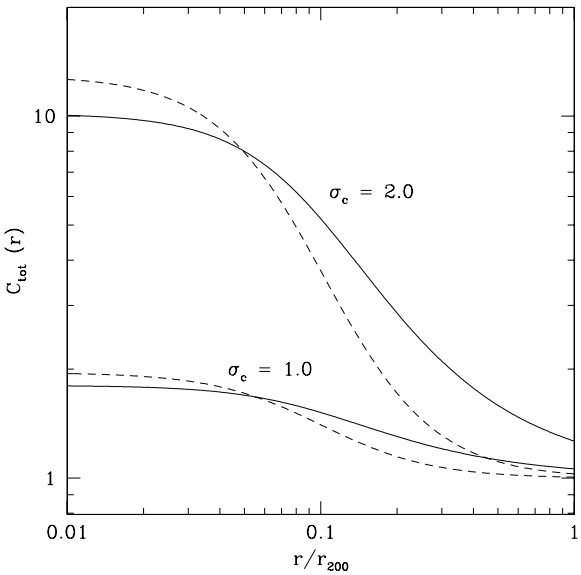

Figure 2. The total mass multiphase correction factor $C_{tot}(r)$, equation (20) is shown as a function of radius, using the same parameters and format as in Figure 1.

The total mass of the cluster within a radius r is determined from the hydrostatic equilibrium, equation (2), when comibined with equations (12)-(16) give

$$M_{\rm tot,m}(r) = -\left(\frac{r^2}{G}\right)\left(\frac{C_P(r)P_s'(r)+P_s(r)C_P'(r)}{C_\rho(r)\rho_s(r)}\right) = \frac{C_P(r)}{C_\rho(r)}M_{\rm tot,s}(r)+\frac{r^2}{G}\frac{k_BT_X}{\mu m_p}\left|\frac{C_P'(r)}{C_\rho(r)}\right|. \quad (19)$$

The total cluster mass for the multiphase model differs from that of the single-phase model by the factor

$$C_{\rm tot}(r) = \frac{C_P(r)}{C_\rho(r)}+\frac{r^2}{GM_{\rm tot,s}(r)}\frac{k_BT_X}{\mu m_p}\left|\frac{C_P'(r)}{C_\rho(r)}\right|. \quad (20)$$

For bremsstrahlung emission ($\alpha \simeq 0.5$), the gas mass is decreased and the total mass increased in the multiphase case, implying the enclosed gas fraction at radius r is lower than that for a single-phase medium by the factor $C_{\rm b}(r) = C_{\rm gas}(r)/C_{\rm tot}(r)$.

Figure 1 plots the correction factor for the cluster gas mass, $C_{\rm gas}$, for a few choices of the controlling parameters σ_c and ϵ. For purposes of illustration, we take structural parameters representative of rich clusters, namely $r_c/r_{200}=0.1$ and $\beta=2/3$ (Neumann & Arnaud 1999), and assume pure bremsstrahlung emission, $\alpha=1/2$. The effect of the radial falloff of the multiphase structure on gas mass estimates is substantial. Density variations with large central rms perturbations $\sigma_c \simeq 2.0$ produce substantial (factor $\sim$3) relative correction to the gas mass in the cluster core, but the effect on the total virial gas mass (mass within r_{200}) is reduced to 25% if $\epsilon = \frac{1}{2}$ and only 10% if $\epsilon = 1$. Degeneracies exist in the virial gas correction factor; a relatively weak multiphase plasma distributed throughout the cluster can produce an effect that is similar to a plasma with strong density variations concentrated toward the center of the cluster (*cf.* $\{\sigma_c, \epsilon\}$ combinations of $\{1, \frac{1}{2}\}$ and $\{2, 1\}$).

The correction factor for the total cluster mass, $C_{\rm tot}$, for the same multiphase parameters is shown in Figure 2. By steepening pressure gradients, the multiphase effects increase the total cluster mass derived from equation (19). Once again, weaker multiphase effects distributed throughout the cluster can yield a total mass within r_{200} that is similar to a cluster plasma with stronger density variations concentrated in the cluster center. However, such concentrated multiphase effects will produce a total mass profile that is steeper (*cf.*(σ_c, ϵ) of $(2, \frac{1}{2})$ *vs.* $(2, 1)$). Observations of strong gravitational lensing could be used to break this parameter degeneracy, to the extent that the hydrostatic assumption is valid in the cluster core.

3 CONSEQUENCES

We now turn to the issue of the effect of multiphase structure on inferred ICM gas fractions and cluster observables. For the latter, we consider the effects of multiphase plasma on a cluster's X–ray spectrum and the Sunvaev-Zel'dovich microwave decrement through a line-of-sight taken through the center of the cluster.

All of the results we discuss assume a standard structure model with core radius for the broadband X–ray emissivity (equation (1)) of $r_c = 0.1r_{200}$, exponent $\beta = 2/3$, and, for creation of X–ray spectra, an emission-weighted X–ray temperature $T_X = 10^8$ K. Unless otherwise stated, we employ a value of $\alpha=0.36$ for the exponent of the plasma emission function, derived from a Raymond-Smith code as described

Table 1. Model Definitions

Label	σ_c	ϵ
SP	0	–
MP-A	0.5	0
MP-B	2.0	0.8
MP-C	1.0	0
MP-D	2.0	0.4
MP-E	2.0	0

below. Since we ignore galaxies in our modeling, the ICM gas fraction is synonymous with the cluster baryon fraction. We use the terms interchageably below, but it must be remembered that the stellar content of cluster galaxies and intracluster light presents an absolute lower limit to the baryon content of clusters.

3.1 Baryon fraction bias

The effects of increased total mass and decreased gas mass shown in Figures 1 and 2 combine multiplicatively to reduce the cluster baryon fraction. The magnitude of the effect within the virial radius is shown in Figure 3, where we show contours of $C_{\rm b}(r_{200})$, the baryon reduction factor, in the $\{\sigma_c, \epsilon\}$ plane.

The baryon reduction effect peaks at high σ_c and low ϵ. At $\epsilon = 0$, the uniform, mulitphase structure of GT96 is recovered, with magnitude

$$C_{\rm b} = \frac{C_\rho^2}{C_{\rm P}} = \exp\Big(\frac{(\alpha-1)(\alpha+6)}{4}\sigma_c^2\Big). \qquad (21)$$

To reduce the baryon fraction by factors $C_{\rm b} \gtrsim 2$ requires density variations of magnitude $\sigma_c \gtrsim 1$.

In the following discussion, we highlight a set of five specific models, listed in Table 1. Models A and B have small ($\sim 20\%$) baryon corrections, models C and D have large baryon bias $C_{\rm b} \sim 2$ and model E is an extreme model in which the baryon fraction is reduced by an order of magnitude.

3.2 Sunyaev-Zel'dovich Effect

The SZ effect is produced by inverse-Compton scattering of cosmic microwave background (CMB) radiation off thermally excited electrons in the hot ICM plasma (see Birkinshaw 1998 for a recent review). We calculate the central Comptonization parameter of the (nonrelativistic) thermal SZ effect

$$y(0) = \int n_e(l)\sigma_T \frac{k_B T(l)}{m_e c^2}\, dl \qquad (22)$$

where the integral dl is along a narrow line of sight through the center of the spherical cluster. Here $n_e = \rho/\mu_e m_p$ is the electron number density and σ_T the Thomson cross section. Since the plasma phases are assumed isobaric, the product $n_e(r)T(r)$ is constant, and no phase integral is necessary in the multiphase case. Deviation of the y–decrement from that of a single-phase plasma is caused by the alteration of the overall pressure profile in the cluster.

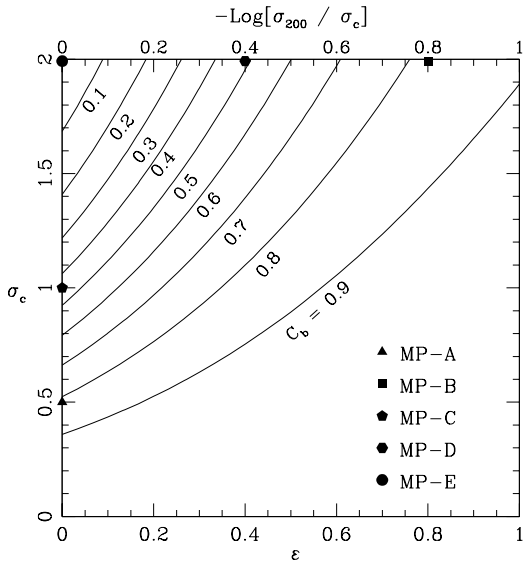

Figure 3. The baryon multiphase correction factor evaluated at the virial radius, $C_b(r_{200})$ is displayed in a contour plot within the ε, σ_c plane. Standard parameters $r_c/r_{200} = 0.1$ and $\beta = 2/3$ are assumed. Labels refer to models whose multi-phase spectra are displayed in Figures 5 and 6.

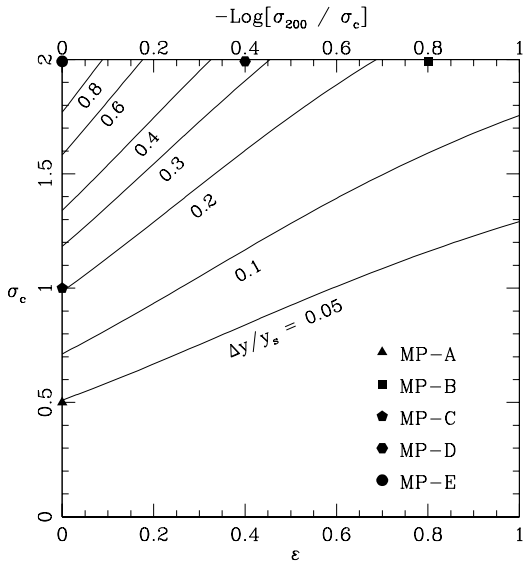

Figure 4. Contours of the fractional increase in central Sunyaev-Zel'dovich decrement for the multiphase models relative to the singe-phase case, assuming $r_c/r_{200} = 0.1$, $\beta = 2/3$ and $\alpha = 0.36$.

The fractional deviation of the central Comptonization parameter $\Delta y/y_s = [y_m(0) - y_s(0)]/y_s(0)$ in the multiphase with respect to the single-phase model is shown in Figure 4. In the case of a uniform, multiphase structure ($\epsilon = 0$), the fractional change in y follows from the pressure correction factor, equation (16),

$$\Delta y/y_s = \exp\Big(\frac{(1-\alpha)(2-\alpha)}{4}\sigma_c^2\Big) - 1. \quad (23)$$

Figure 4 shows data for the case $\alpha = 0.36$, approximately the slope of the $2-10$ keV luminosity versus temperature, derived from a Raymond–Smith plasma code assuming a one–third solar abundance of metals. Similar values result for the case $\alpha = 0.5$.

The two models with 20% baryon diminution have modest, but potentially discernable, SZ effects. Model A has a central decrement enhanced by 10% while model B is enhanced by 25% over the single-phase case. The latter is similar to the 30% effect for model C, one of the large baryon fraction diminution models. The other factor 2 baryon fraction model — model D — has a central value of y increased by $\sim 50\%$ over the standard β–model . The extreme model E has a signal enlarged by a factor 2 over the standard case.

Even in the single-phase case, there is inherent uncertainty in predicting the SZ effect amplitude from X-ray observations which arises from uncertainty in the physical distance to the cluster. At low redshifts, the distance error is completely due to uncertainty in the Hubble constant. Given a cluster with fixed X–ray properties, a fractional deviation in central SZ decrement $\Delta y/y_s$ due to a multiphase medium could, instead, be interpreted as a distance effect. This would imply a fractional error in the Hubble constant

$$\Delta H_0/H_0 \;=\; -2\;\Delta y/y_s. \quad (24)$$

For example, in a universe with true Hubble constant of 65 km s^{-1} Mpc^{-1}, observations of a multiphase model A cluster would yield a value 52 km s^{-1} Mpc^{-1} and model B would produce an estimate of 42. The other highlighted models would produce even lower estimates of H_0.

Note that this result has the *opposite* sense of correction for the SZ decrement compared to other estimates of the SZ effect with multiphase gas (*e.g.*. Holzapfel et al. 1997). This is because the gas pressure for isobaric density fluctuations is greater than that for a single-phase medium, whereas other models with adiabatic density fluctuations, such as those present in SPH calculations without cooling (Inagaki, Suginohara & Suto 1995), have a pressure lower than that of the single-phase gas.

3.3 X-ray spectra

Spectroscopic analysis of the X–ray emission provides an alternative, independent diagnostic of multiphase structure. We calculate expected X–ray spectra from the multiphase plasma in two ways. We first consider a simple model for the X–ray bremsstrahlung continuum from the cluster, using an emission function of a purely hydrogen plasma, with $\varepsilon(E,T) \propto T^{-\frac{1}{2}} e^{-\frac{E}{kT}}$ and a Gaunt factor of unity. The plasma emission function is then $\Lambda(T) = K_0 T^{1/2}$, with K_0 an arbitrary normalization amplitude. Second, a more detailed spectrum is calculated, using the Raymond-Smith plasma emission code (Raymond and Smith 1977) with metal abundances one-third of the solar value (Allen 1973). The former approach highlights continuum behavior while the latter allows the study of the behavior of X–ray lines between $0.5-9$ keV.

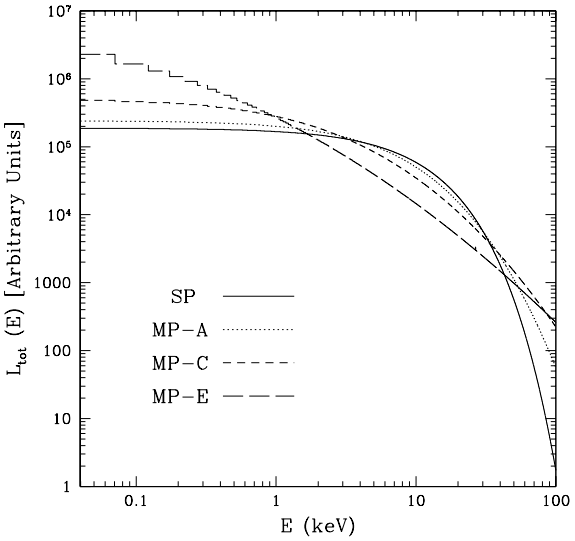

Figure 5. X-ray continuum emission for different multiphase models listed in Table 1. A value of $\alpha = 0.5$ is assumed. All models have the same emission weighted temperature of 10^8 K in the spectral region shown.

We generate the composite spectrum emitted by the multiphase cluster atmosphere by numerically integrating the weighted emission over the density distribution at a particular radius, then intergrating over the cluster volume $V = \frac{4\pi}{3} r_{200}^3$. Gas beyond the virial radius r_{200} is ignored.

The appearance of the continuum plasma X–ray emission in the multiphase case can differ substantially from that of the isothermal, single-phase plasma. In Figure 5, we show the $0.05-100$ keV bolometric X–ray spectra of three multiphase models (A, C and E) along with the single-phase case. All spectra are normalized to yield the same emission weighted temperature of 10^8 K. We assume all phases are optically thin. The most important effect on the spectra is the appearance of both low-energy ($E \ll k_B T_X$) and high-energy ($E \gg k_B T_X$) enhancements of the spectrum with increasing magnitude of multiphase effects. This shape change arises from the blending of gas at temperatures both below and above the fiducial 10^8 K value. In the limit of extreme multiphase strength (model E), the bremsstrahlung spectrum approaches power-law like behavior.

A more complete X-ray spectrum of clusters is code. In particular, the use of such a code allows invesigation of line emission as a diagnostic of multiphase structure.

Figure 6 shows the simulated emission, derived from a Raymond-Smith code, between $0.1-15$ keV photon energies for a plasma with an assumed metallicity equal to one–third of solar abundance. Along with the rise of the low-energy continuum, the other prominent effect of increased multiphase structure is the strengthening of low-energy (~ 1 keV) emission lines. To highlight line versus continuum effects, we plot both zero and one–third solar metallicity predictions for the emission for each model shown.

The complex of lines between 0.5 and 1.5 keV presents

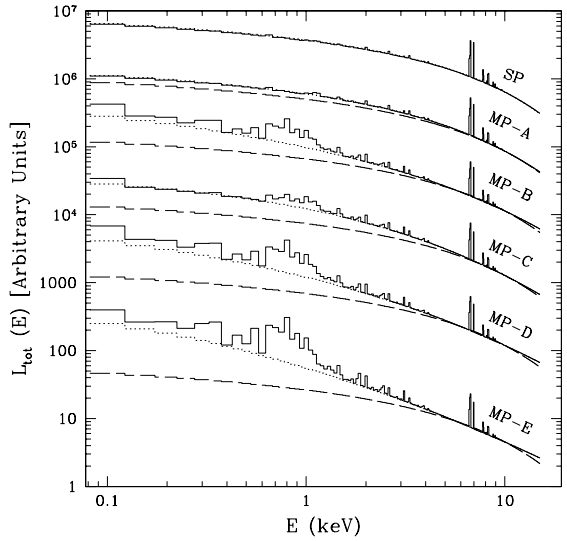

Figure 6. X-ray spectra for different multiphase models derived from a Raymond-Smith code. All models have the same emission weighted temperature of 10^8 K in the $2-10$ keV region. The luminosity of each model is displaced vertically by arbitrary amounts for clarity. Solid lines assume a one–third solar abundance plasma while dotted lines show the multiphase emission assuming zero metallicity. For reference, long dashed lines show the X–ray spectrum of the single-phase cluster with no metal abundances.

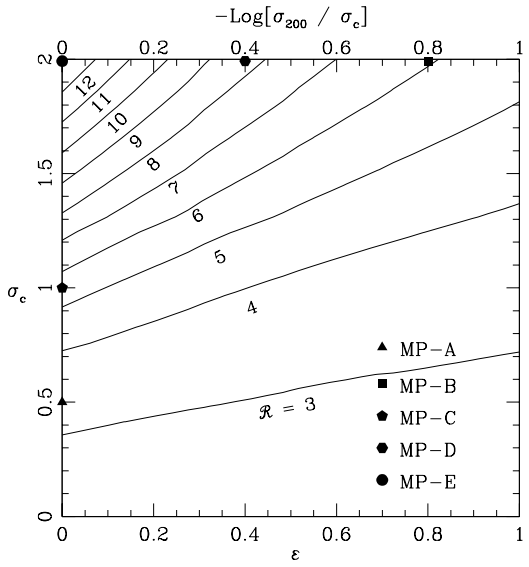

Figure 7. Contours of constant hardness ratio $\mathcal{R}$, equation (25).

a useful diagnostic for multiphase structure. Included in this region of the spectra are the Fe L-shell lines, as well as H-like and He-like emission from N, O, Ne and Mg. For example, weak baryon bias models (A and B) are readily distinguished by this emission signature, as are models the more strongly multiphase models, C and D.

In contrast to the low energy lines, the strength of the 7 keV iron complex is almost unaffected by multiphase structure. These lines originate in hot phases very close to the fiducial temperature of 10^8 K. The emission weighted temperature constraint imposed on the models requires that the contribution to the total emission from phases near the fiducial temperature cannot vary by large factors. Hence the hot emission lines do not vary significantly among the multiphase models.

Given the very different behavior of the low and high energy line emission, we investigate the behavior of a hardness ratio

$$\mathcal{R} \;=\; \frac{L_{tot}[0.6-1.5\ \mathrm{keV}]}{L_{tot}[6.6-7.5\ \mathrm{keV}]} \qquad (25)$$

in the multiphase model plane. For the single phase case, $\mathcal{R}=2.69$. Contours of constant $\mathcal{R}$ in the $\{\sigma_c,\epsilon\}$ plane are shown in Figure 7. From this figure, it is clear that even moderate signal-to-noise spectra could produce useful constraints among models with similar baryon fraction correction factors. Models A and B differ in $\mathcal{R}$ by nearly a factor 2. Models B and C are nearly degenerate in this measure, but inspection of Figure 6 shows that model C is more continuum dominated at low energies while model B has a larger line contribution.

3.4 Limiting the baryon fraction bias

The concluding sentence of GT96 expresses a view "that the intracluster medium is much more complex than most people have hitherto assumed and that there is sufficient uncertainty in its modeling to permit a critical density, Einstein-deSitter universe". Within the context of the expanded version of their model which we develop here, we can ask whether this opinion is supported by recent data.

A number of high quality measurements of the Hubble constant from SZ and X–ray observations have been made recently (Myers et al. 1997; Birkinshaw & Hughes 1994; Jones 1995; Hughes & Birkinshaw 1998; Holzapfel et al. 1997). Hughes & Birkinshaw (1998) present an ensemble value $H_0 = 47 \pm 7$ km s^{-1} Mpc^{-1} from these studies. For a true value $H_0 = 65$ km s^{-1} Mpc^{-1}, supported by Type Ia supernovae (Hamuy et al. 1995; Riess et al. 1996), expanding photosphere of Type II supernovae (Schmidt et al. 1994) gravitational lens time delays (Kundi et al. 1997; Schechter et al. 1997), this ensemble average is low by 28%. Assuming that a multiphase structure is at least partly responsible for this biased estimate — other effects may lead to an underestimate at the $\sim 5-10\%$ level (Cen 1998) — then a bound on the SZ decrement enhancement $\Delta y/y_s \lesssim 0.14$ results. Comparing the contours in Figures 3 and 4, this limit restricts baryon fraction diminution factors to be modest, $0.75 \lesssim C_{\rm b} \leq 1$.

3.5 Caveats and extensions

The model we present contains a number of simplifying assumptions. It is important to note that the model is, in prin-

ciple, falsifiable. Given a known Hubble constant, likelihood analyses of SZ observations and X–ray spectra will independently identify preferred regions in the $\{\sigma_c, \epsilon\}$ plane. If these regions are consistent, the observations can be combined to yield a best estimate location $\{\hat{\sigma}_c, \hat{\epsilon}\}$, and an estimate of the baryon fraction bias $C_{\rm b}$ (Figure 3). Inconsistent constraints may imply a need to relax one or more of the following assumptions.

Lack of spherical symmetry. With rare exceptions, cluster X–ray images are close to round. Most have axial ratios $b/a \gtrsim 0.8$ (Mohr et al. 1995). Such small deviations from spherical symmetry lead to scatter, but little bias, in determinations of H_0 from SZ+X–ray analysis (Sulkanen, 1999). Given supporting evidence for a multiphase ICM in a cluster of moderate ellipticity, the spherical model introduced here could be extended to prolate or oblate spheroids. A more profitable approach might be to include multiphase structure in the deprojection method discussed by Zaroubi et al. (1998).

Non-isothermal emission weighted temperature profiles. There is indication from ASCA observations (Markevitch et al. 1998) that the emission weighted ICM temperature declines substantially within the virial radius. However, ROSAT colors rule out a temperature drops of 12/20% for 5/10 keV clusters within one-third of r_{200} (Irwin, Bregman & Evrard 1999). It is straightforward to include a radial temperature gradient $T_X(r)$ into the analysis, entering into the definition of the pressure profile, equation 10.

Non-lognormal distribution of density fluctuations. The chosen form of the density distribution is motivated by simplicity and by the observation that non–linear gravity on a Gaussian random density field characteristically generates a log-normal pdf (Cole & Weinberg 1994). The results are sensitive to low order moments of the density distribution. We await observations and future numerical simulations including cooling and galaxy-gas interactions in a three-dimensional setting to shed light on the appropriate form of the density fluctuation spectrum.

Non-isobaric equation of state. This may be the most readily broken of our model assumptions. The cluster environment is very dynamic. During large mergers, the behavior of the gas in the inner regions of infalling subclusters is essentially adiabatic (Evrard 1990; Navarro, Frenk & White 1993). During quiescent periods between mergers, a cluster atmosphere may stabilize and develop the assumed isobaric perturbations during a cooling flow phase (Thomas et al. 1986). In the transition period, isobaric perturbations in the core may co-exist with adiabatic perturbations near the virial radius. Empirical constraints will come from improved spectroscopic imaging.

Binding mass estimates under hydrostatic equilibrium. As noted in §2.2, the radial dependence of our model multiphase distribution can lead to a total mass profile $M_{tot,m}(r)$ that is steeper than that determined for a single-phase gas. Galaxy cluster lensing observations could be used to test the mass distribution predicted by multiphase models (see Figure 2). This provides another independent constraint on the admissable region of the multiphase $\{\sigma_c, \epsilon\}$ plane.

4 SUMMARY AND DISCUSSION

We present a spherically symmetric, multiphase model of the intracluster medium in galaxy clusters. The model assumes existence of a lognormal distribution of isobaric density and temperature fluctuations at any radius. The radially dependent variance of the density fluctuations $\sigma^2(r)$ is subject to two empirical constraints : 1) that the broadband X–ray emissivity profile matches observations and 2) that the X–ray emission-weighted temperature is constant with radius.

We calculate the bias introduced in cluster gas mass fraction estimates when a single-phase model is a applied to a multiphase atmosphere. As derived by GT96, the standard analysis of the X–ray observations with a single-phase assumption will overestimate the baryon fraction in the multiphase case. Examining observable effects on the central Sunyaev-Zel'dovich decrement as well as X–ray spectroscopy, we demonstrate how, within the context of this model, the bias can be recovered by existing and future observations.

Large values of the clumping factor $\mathcal{C}$, hence large reduction in the cluster baryon fraction are not favored by current observations. Models with high values of σ_c produce a nearly power-law X–ray bremsstrahlung continuum and bias estimates of the Hubble constant. An ensemble mean value 47 ± 7 km s^{-1} Mpc^{-1} (Hughes & Birkinshaw 1998) arising from recent SZ+X–ray analysis, when compared to an assumed value of 65 km s^{-1} Mpc^{-1}, suggests clumping only overestimates ICM gas fractions by $\lesssim 20\%$.

Spatially resolved X–ray spectroscopy, particularly of line emission in cooler region (0.1-3keV), will provide tests of multiphase model. Data from the upcoming AXAF and XMM missions will be particularly valuable.

ACKNOWLEDGMENTS

This work is supported by the National Science Foundation through the 1998 physics REU summer program at the University of Michigan and through grant AST-9803199. We acknowledge NASA support through grant NAG5-7108 and NSF through grant AST-9803199. M.E.S. thanks NASA's Interagency Placement Program, the University of Michigan Department of Astronomy, and the University of Michigan Rackham Visiting Scholars Program.

REFERENCES

Allen, C. W., 1973, Astrophysical Quantities (3rd ed.; London: Athlone).

Birkinshaw, M., 1998, Physics Reports, in press (astro-ph/9808050).

Birkinshaw, M. & Hughes, J. P., 1994, ApJ, 420, 33B.

Cavaliere, A. & Fusco-Fermiano, R., 1976, A&A, 137-144.

Cen, R. 1998, ApJ, 498, L99.
Cole, S., Fisher, K. B. & Weinberg, D. H, 1994 MNRAS, 267, 785C.
David, L. P., Jones, C. & Forman, W., 1995, ApJ, 445, 578.
Eke, V. R., Navarro, J. F. & Frenk, C. S., ApJ, 503, 569.
Evrard, A. E. 1990, in Clusters of Galaxies, eds. W. Oegerle, M. Fitchett, & L. Danly, Cambridge: Cambridge University Press, 287.
Fabian A.C., Crawford C.S., Edge A.C., Mushotzky R.F., 1994, MNRAS, 267, 779
Gunn K.F. & Tomas P.A., 1996, MNRAS, 281, 1133.
Holzapfel, W.L., Arnaud, M., Ade, P.A.R., Church, S.E., Fischer, M.L., Mauskopf, P.D., Rephaeli, Y., Wilbanks, T.M. & Lange, A.E. 1997, ApJ, 480, 449.
Hughes, J. P. & Birkinshaw, M., 1998, ApJ, 501, 1.
Inagaki, Y., Suginohara, T. & Suto, Y. 1995, PASJ, 47, 411.
Irwin, J. A., Bregman, J. N. & Evrard, A. E., 1998, AAS, 193.3802I.
Irwin, J.A., Bregman, J.N. & Evrard, A.E. 1999, ApJ, in press (astro-ph/9901406).
Jones, M. 1995, Astrophys Lett & Comm, 32, 347.
Kundic, T. et. al., 1997, ApJ, 482, 75K.
Markevitch, M. et. al., ApJ, 1998, 503, 77M.
Mamuy, M. et. al., 1995, AJ, 109, 1H.
Mohr, J.J. Mathiesen, B. & Evrard, A.E. 1999, ApJ, in press (astro-ph/9901281).
Myers, S. T., Baker, J. E., Readhead, A. C. S., Leitch, E. M. & Herbig, T., 1997, ApJ, 485, 1M.
Navarro, J. F., Frenk, C. S. & White, S. D. M., 1994, MNRAS, 267L, 1N.
Neumann, D.M. & Arnaud, M. 1999, astro-ph/9901092.
Nulsen, P.E. J., 1986, MNRAS, 221, 377.
Raymond, J. C. & Smith, B. W., 1977, ApJS, 35, 419.
Riess, A. G., Press, W. H. & Kirshner, R. P., 1996, ApJ, 473, 88R.
Schechter, P. L. et. al., 1997, ApJ, 475L, 85S.
Schmidt, B. P. et. al., 1994, ApJ, 432, 42S.
Sulkanen, M.E. 1999, ApJ, submitted.
Thomas, P., 1988 MNRAS, 235, 315T.
Thomas, P. A., Fabian, A. C., Arnaud, K. A., Forman, W. & Jones, C., 1986, MNRAS, 222, 655T.
White, D. A. & Fabian, A. C., 1995, MNRAS, 72.
White S.D.M., Navarro J.F., Evrard A.E., Frenk C.S., 1993, Nature, 366, 429.
Zaroubi, S., Squires, G., Hoffman, Y. & Silk, J., 1998, ApJ, 500L, 87Z.